

# Computer Simulation of Fresnel Diffraction from Triple Apertures by Iterative Fresnel Integrals Method

Fatema Hamid Al-Saiari<sup>1</sup>, S.M. Mujibur Rahman<sup>2</sup>, Kazi Monowar Abedin<sup>3\*</sup>

Physics Department, College of Science, Sultan Qaboos University, P.O. Box 36, Postal Code 123, Muscat, Oman

\*Corresponding author, permanent Address: Department of Physics, University of Dhaka, Dhaka-1000, Bangladesh

<sup>1</sup>alkhatab.af@gamil.com; <sup>2</sup>mujib@squ.edu.om; <sup>3</sup>abedinmonowar@yahoo.com

**Abstract-**The Iterative Fresnel Integrals Method (IFIM) has been applied for the simulation and generation of the complete near-field Fresnel diffraction images created by triple apertures for the first time. The simulation can be performed in any PC using an included MATLAB program. Necessary formalism has been derived and simulation algorithm has been developed for this application. An interesting combination of interference effects with Fresnel diffraction has been observed in the simulation images. Transition to the expected Fraunhofer diffraction pattern from Fresnel diffraction for triple apertures is also observed by the simulations. The program can serve as a useful tool to study the complex phenomenon of Fresnel diffraction from triple apertures.

**Keywords-**Fresnel Diffraction; Triple Aperture; Computer Simulation; Iterative Fresnel Integrals Method; Virtual Experiment

## I. INTRODUCTION

In Optics, diffraction is a subject of recurring importance, both from a theoretical and experimental point of view [1-3]. Diffraction phenomena can be grossly classified into two types, namely: Fresnel and Fraunhofer. Of these two, the Fresnel or near-field diffraction is relatively more complicated than the Fraunhofer, or far-field diffraction. No exact analytical solution of Fresnel diffraction can be found even in the simplest cases. For example, even for a simple rectangular or circular aperture, no analytical solution can be obtained for Fresnel diffraction. In this case, a solution can be obtained in terms of non-analytical integrals known as Fresnel integrals [2,3]. Even then, visualizing the complicated Fresnel diffraction can be a difficult task. Usually some visualization tools, such as Cornu Spiral, are necessary, and even if it's used, the complicated diffraction pattern observed is not easy to explain and interpret [2].

We previously introduced a new method of calculation of the complete Fresnel diffraction pattern from rectangular-shaped apertures by the Iterative Fresnel Integrals Method (IFIM). The technique has been applied to a single rectangular aperture [4], double apertures and its derivatives [5] and a tilted aperture [6]. Instead of the usual methods of calculation of Fresnel diffraction from apertures, which generally uses FFT-based algorithms [7-9], the IFIM method uses repeated calculation of Fresnel cosine and sine integrals and virtual displacements of the aperture [4]. The method provides a very intuitive method of calculation of the diffraction pattern, and two-dimensional images can be directly generated by the method in any arbitrary experimental configurations, such as for any given aperture size, illumination wavelength, and aperture-screen distances. The algorithm was implemented in MATLAB, and the codes can be executed in any PC or laptop

in a reasonable amount of time, with execution times less than a minute in most cases. Implementation of the codes in other languages, such as Mathematica or MathCad is also possible.

In this paper, we extend the IFIM technique to a triple aperture. We first derive the basic equation to describe the electric field or intensity due to the triple aperture, and then formulate the detailed algorithm for the computation process. The algorithm is then implemented in MATLAB. We present output images from the MATLAB program for typical cases of the triple aperture problem. Finally, discussions are made and conclusions are drawn in the final sections.

## II. THEORETICAL CONSIDERATIONS

To understand the underlying theory of Fresnel diffraction from a triple aperture, let us first consider the case of a single aperture. Light of wavelength  $\lambda$  emitted from a point source S is diffracted by a rectangular aperture of dimension  $a \times b$  located at a distance  $p_0$  from it (Fig.1). The diffracted light is observed on the observation plane (or screen) placed a distance  $q_0$  away. For convenience, the coordinate systems on the aperture and on the image planes are chosen to be centered on the optical axis passing through the center of the aperture and normal to it, and are denoted by  $(y, z)$  and  $(Y, Z)$  axes, respectively. The Huygens-Fresnel principle is then invoked to calculate the total electric field at any given point of the image plane  $(Y,Z)$  by summing up the contributions, taking into account both amplitude and phase, of all the elementary wavelets emitted by different area elements inside the clear rectangular aperture.

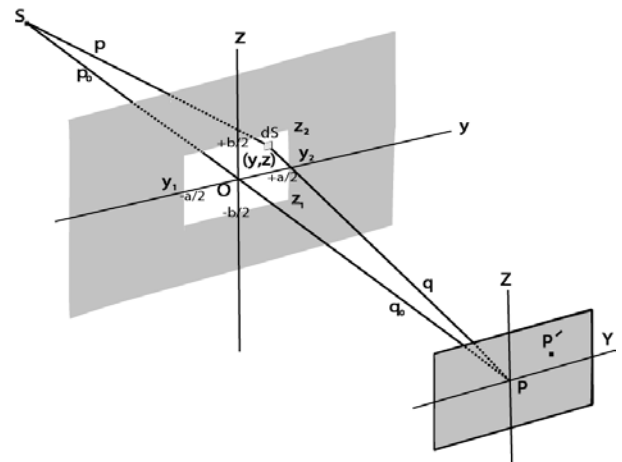


Fig. 1 Basic configuration of Fresnel diffraction from a rectangular aperture

The contribution to the complex electric field at the point P (located at the origin of the image plane or screen) due to

waves emitted by the surface element  $dS$  located on the aperture is given by [2, 3]

$$dE = \frac{\epsilon_0 K(\phi)}{pq\lambda} \exp[j\{k(p+q) - \omega_0 t\}] dS \quad (1)$$

where  $\epsilon_0$  is the electric field of the source,  $k$  is the wavenumber ( $2\pi/\lambda$ ) and  $K(\phi) = \frac{1}{2}(1 + \cos \phi)$  is the obliquity factor [2, 6], where  $\phi$  is the angle between the normal to the surface element  $dS$  and the direction of wave propagation. The obliquity factor  $K(\phi)$  takes into account the decrease of intensity for secondary Huygens wavelets emitted from  $dS$  in an oblique direction. In our case, since  $q_0$  is much larger than the dimensions of the aperture,  $\phi$  is quite small, and  $K(\phi)$  is nearly unity.

The net electric field at P due to the entire tilted aperture is obtained by summing up the contributions  $dE$  over the entire rectangular aperture,

$$E_P = \int_{aperture} \frac{\epsilon_0 K(\phi)}{pq\lambda} \exp[j\{k(p+q) - \omega_0 t\}] dS. \quad (2)$$

By integrating the contributions of the Huygens wavelets over the area of the entire aperture, it is shown in textbooks [2, 3] that the total electric field at P is given by

$$E_P = \frac{E_u}{2} [C(u) + iS(u)]_{u_1}^{u_2} [C(v) + iS(v)]_{v_1}^{v_2} \quad (3)$$

where  $E_u$  is the unobstructed electric field at P (i.e. the electric field that would have existed if the aperture were absent), and  $C(u)$  and  $S(u)$  are the Fresnel cosine and sine integrals, defined by,

$$C(w) = \int_0^w \cos(\pi w'^2 / 2) dw' \quad \text{and} \\ S(w) = \int_0^w \sin(\pi w'^2 / 2) dw'. \quad (4)$$

Here  $w$  represents either of the two dimensionless variables  $u$  or  $v$ , being defined as,

$$u = y \sqrt{\frac{2(p_0 + q_0)}{\lambda p_0 q_0}}, \quad v = z \sqrt{\frac{2(p_0 + q_0)}{\lambda p_0 q_0}}. \quad (5)$$

The variables  $u$  and  $v$  are obviously proportional to Cartesian coordinates  $y$  and  $z$ . Specifically, the limits  $u_1, u_2, v_1, v_2$  correspond to the values of  $y_1, y_2, z_1, z_2$ , respectively.

The intensity at P is given by the square of  $E_P$ , appearing in Eq.(3) i.e., by,

$$I_P = \frac{I_0}{4} \{ [C(u_2) - C(u_1)]^2 + [S(u_2) - S(u_1)]^2 \} \times \\ \{ [C(v_2) - C(v_1)]^2 + [S(v_2) - S(v_1)]^2 \}. \quad (6)$$

Here,  $I_0$  is the unobstructed intensity corresponding to  $E_u (I_0 = E_u^2)$ .

Let us now consider the much more complicated case of a triple aperture. As before in the single aperture case, we assume that the aperture is centered on the  $yz$  coordinate system, i.e., the origin of the coordinate system O is located at the exact center of the triple aperture (Fig. 2). The two edges

of the central aperture are then located at  $y=a/2$  and  $y=-a/2$  respectively, and the edges of the right aperture is located at  $y=a/2+b$  and  $y=3a/2+b$  respectively. Similarly, the edges of the left aperture are located at  $y=-a/2-b$  and  $y=-3a/2-b$ . In this notation, the aperture width is  $a$  and center-to-center aperture separation is  $(a+b)$ . The upper and lower edges of the apertures are located at  $z=c$  and  $z=-c$  respectively.

Under illumination from the source, the total electric field at the center P of the image plane consists of three contributions: one from right aperture, one from the central aperture, and the one from the left aperture. The total electric field contribution from the right aperture is given, in analogy to Eq. (3), by

$$E_{PR} = \frac{E_u}{2} [C(u) + iS(u)]_{u_1}^{u_2} [C(v) + iS(v)]_{v_1}^{v_2} \quad (7)$$

Here, the limits  $u_1$  and  $u_2$  are the values of the dimensionless variable  $u$  corresponding to two edges of the right aperture, i.e. for  $y_1=a/2+b$  and  $y_2=3a/2+b$ , respectively. Similarly, the limits  $v_1$  and  $v_2$  are the values of the dimensionless variable  $v$  corresponding to the lower and the upper edges of this aperture i.e. for  $z_1=-c$  and  $z_2=c$  respectively.

The total electric field contribution by the central aperture is similarly given by

$$E_{PC} = \frac{E_u}{2} [C(u) + iS(u)]_{u_3}^{u_4} [C(v) + iS(v)]_{v_1}^{v_2} \quad (8)$$

where  $u_3$  and  $u_4$  are the values of  $u$  corresponding to two edges of the central aperture, i.e. for  $y_3=-a/2$  and  $y_4=a/2$  respectively. The values  $v_1$  and  $v_2$  are the same as in Eq. (3) or Eq. (7).

The total electric field contribution by the left aperture is similarly given by

$$E_{PL} = \frac{E_u}{2} [C(u) + iS(u)]_{u_5}^{u_6} [C(v) + iS(v)]_{v_1}^{v_2} \quad (9)$$

where  $u_5$  and  $u_6$  are the values of  $u$  corresponding to two edges of the central aperture, i.e. for  $y_5=- (3a/2+b)$  and  $y_6=- (a/2+b)$ , respectively. The values  $v_1$  and  $v_2$  are the same as in Eq. (7) and Eq. (8).

The total electric field at P contributed by the triple aperture is given by the arithmetic sum of the three complex amplitudes from the left, centre and right apertures; i.e. by,

$$E = E_{PR} + E_{PC} + E_{PL} \\ = \frac{E_u}{2} \{ [C(u) + jS(u)]_{u_1}^{u_2} + [C(u) + jS(u)]_{u_3}^{u_4} + \\ [C(u) + jS(u)]_{u_5}^{u_6} \} \times [C(v) + jS(v)]_{v_1}^{v_2} \quad (10)$$

The intensity at P is proportional to  $(EE^*)$ , i.e.,

$$I_P = \frac{I_0}{4} \{ [C(u_2) + C(u_4) + C(u_6) - C(u_1) - C(u_3) - C(u_5)]^2 \\ + [S(u_2) + S(u_4) + S(u_6) - S(u_1) - S(u_3) - S(u_5)]^2 \} \times \\ \{ [C(v_2) - C(v_1)]^2 + [S(v_2) - S(v_1)]^2 \}. \quad (11)$$

Here  $I_0$  denotes the intensity of the unobstructed wave, i.e.  $I_0 = E_u^2$ .

If  $b$  is set to zero, then we have a single aperture of width  $3a$ . In that case, both  $u_4 = u_1$  and  $u_6 = u_3$ , and, hence only  $C(u_2)$ ,  $C(u_5)$ ,  $S(u_2)$ ,  $S(u_5)$  terms in the first factor of Eq. (11) are non-zero, with  $u_2=3a/2$  and  $u_5=-3a/2$ . In this case, Eq. (11) reduces

to Eq (6) for a single aperture with an aperture width of  $3a$ , as it must.

From Eq.(10) or Eq.(11), it is clear that the calculation of electric field or intensity at a point P requires, in general, the evaluation of 16 Fresnel integrals. 12 of these involve the argument in  $u$  (or  $y$ ) only, and the remaining 4 in  $v$  (or  $z$ ) only. These equations are the basis of calculation of the complete intensity distribution of the Fresnel diffraction pattern from a triple aperture, as will be seen in the next section. Either of these two equations can be used, but in this work Eq. (10) was chosen to calculate firstly the electric field, and then the intensity was calculated by taking the square of it. These equations have two factors, the first factor involves only the  $u$  (or  $y$ ) coordinate and expresses the dependence of electric field or intensity in the  $y$  direction. The second factor involves only the  $v$  (or  $z$ ) coordinate and expresses the dependence of electric field or intensity in the  $z$  direction.

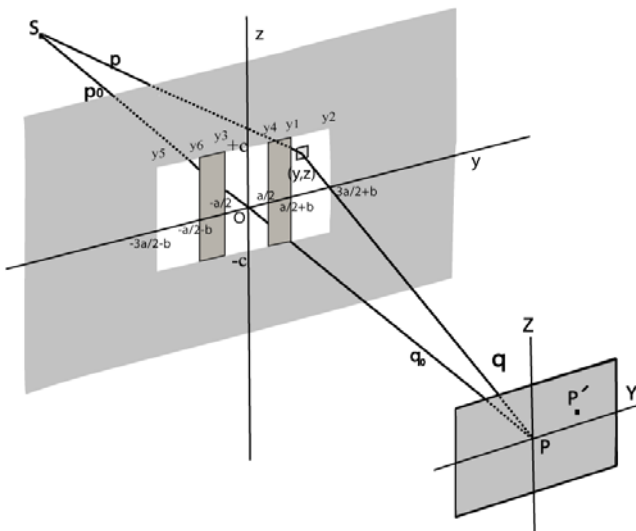


Fig. 2 Configuration of the triple-aperture problem for Fresnel diffraction.  $a$  is the individual aperture width and  $(a+b)$  is the aperture separation.

### III. SIMULATION TECHNIQUE

Eq. (10) and Eq. (11) describe the electric field and the intensity at P, respectively. In order to describe these for an off axis point P', a method outlined in [4] and [5] was used. The observation screen and SOP line were fixed. Then instead of moving P, the aperture in  $yz$  plane was moved in opposite direction, so that the relative position of the aperture is this new position and point P remains unchanged. We then calculate the electric field at P instead of at P'. Point P' will see a new set of values for  $y$ 's and  $z$ 's (and therefore for  $u$ 's and  $v$ 's). For example, to find the intensity at point P' 1mm to the left of P, the screen was kept undisturbed and the aperture was moved 1mm rightwards, and the intensity at P in this configuration is calculated instead of at P'. Consequently, the point P will now see a new set of values for  $y_1, y_2, y_3, y_4, y_5$  and  $y_6$  and therefore, for  $u_1, u_2, u_3, u_4, u_5$  and  $u_6$  in Eq. (10) and Eq. (11). In principle, the electric field and the intensity at any point P' on the image plane can be found in this way by making appropriate translations of the aperture in the  $y$  and  $z$  directions, and in Eq. (10) or Eq. (12), substituting correspondingly a new set of values of  $u$  and  $v$  limits.

The flow chart of the algorithm is shown in Fig. 3. For calculation of the electric field distribution using Eq. (10) at all the points (pixels) on the image plane, a large number of the Fresnel cosine and sine integrals will need to be evaluated

efficiently. This is accomplished in the MATLAB program using the special functions *mfun* ('FresnelC', *i:s:f*) and *mfun* ('FresnelS', *i:s:f*). For example, the MATLAB statement  $R=mfun('FresnelC', i:s:f)$  generates an array R of

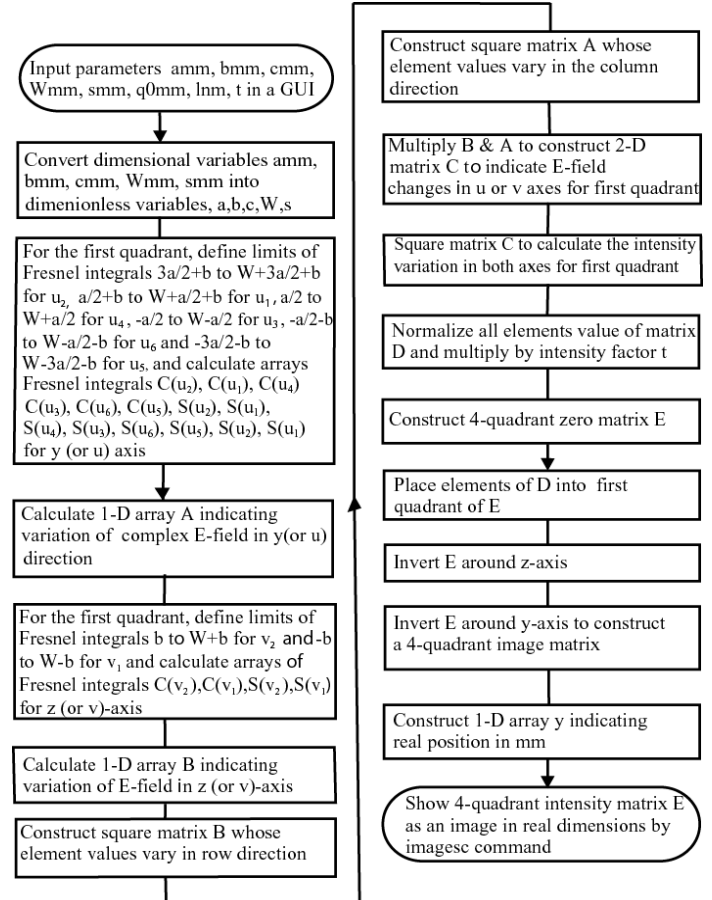


Fig. 3 Flow chart of the algorithm for the triple aperture problem

the Fresnel cosine integrals with arguments starting from  $i$  and ending in  $f$ , with a step size  $s$ . Since the triple aperture is symmetrical about the  $y$  and  $z$  axes, the Fresnel diffraction pattern generated by it will obviously be symmetrical about the  $Y$  and  $Z$  axes in the image plane. Therefore, by using this inversion symmetry around  $Y$  and  $Z$  axes, the amount of calculation can be reduced to one-fourth. Therefore, the diffraction image in only one quadrant (e.g. the first) in the  $YZ$  plane needs to be generated, and then the image in the second quadrant can be generated by simply inverting it around the  $Z$ -axis. Another inversion around the  $Y$ -axis of these two image quadrants will produce the images in the third and fourth quadrants.

As shown in Fig. 4, the aperture was displaced (virtually) by an amount  $W$ , and the extreme limits of the edges of the displaced aperture were determined and compared to the corresponding limits for the undisplaced aperture to find the range of  $u$  and  $v$  values. When the aperture was moved by  $W$  to the left, the ranges for the six edges of the triple aperture will be established as:  $(3a/2+b)$  to  $(W+3a/2+b)$  for  $y_2$ ,  $(a/2+b)$  to  $(W+a/2+b)$  for  $y_1$ ,  $(a/2)$  to  $(W+a/2)$  for  $y_4$ ,  $(-a/2)$  to  $(W-a/2)$  for  $y_3$ ,  $(-a/2-b)$  to  $(W-a/2-b)$  for  $y_6$  and  $(-3a/2-b)$  to  $(W-3a/2-b)$  for  $y_5$ . Arrays of both the Fresnel cosine and sine integrals need to be calculated corresponding to these six ranges by the *mfun* statements. By using these 12 arrays,

the electric field or intensity dependence in the  $y$  ( $u$ ) direction can be calculated (see Eq. 10 or Eq. 11). Following

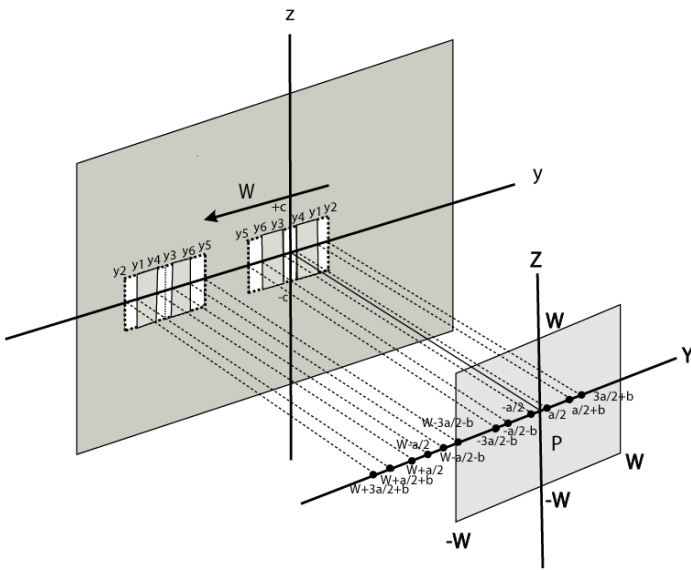


Fig. 4 Apparent limits of the displaced triple aperture seen from the observation area.

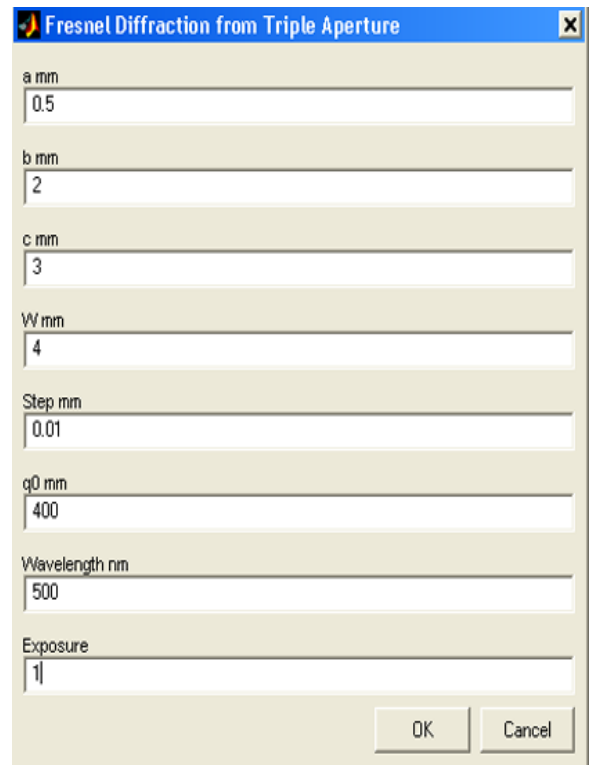
a similar procedure for the entire aperture, i.e. by moving the aperture by  $W$  downwards, the  $z_1$  and  $z_2$  ranges are determined:  $c$  to  $(W + c)$  for  $z_2$  and  $-c$  to  $(W - c)$  for  $z_1$ . Four arrays of Fresnel integrals are to be evaluated for these two ranges, providing numerical values for the calculation of the second factor in Eq. (10).

After the initial parameters to the program are input through a GUI (Graphical User Interface) generated in lines 1-2 of the program, the dimensionless quantities corresponding to aperture dimensions  $a$ ,  $b$  and  $c$ , step size  $s$  and image area size  $W$  are calculated in lines (4-5) of the program. The step size  $s$  determines the resolution of the simulated images, since the number of pixels in the image is given by  $2W/s \times 2W/s$ . The 12 Fresnel integrals arrays for the  $u$  (or  $y$ ) dimension are evaluated in lines (6-17). In line 18, the electric field in  $y$  ( $u$ ) is calculated in complex form, corresponding to the first complex factor in Eq. (10). In the next four lines, the Fresnel cosine and sine integrals are evaluated for the  $z$  (or  $v$ ) dimension. Next, in line 23, the second complex electric field in  $v$  is calculated, corresponding to the second factor in Eq. (10). In the next lines, the matrix  $C$ , which contains the complex electric field variation in both  $u$  and  $v$  directions, is constructed. Finally, by squaring it, the matrix  $D$ , which contains the intensity variations for the first quadrant of the image plane, in both  $y$  and  $z$ , is calculated (line 26). The elements of this matrix then normalized (line 27), and the complete  $E$  matrix for the full image plane intensity distribution is constructed by inverting  $D$  twice (lines 30-38). Finally, the image is displayed as a greyscale image by the `imagesc` command (line 40). The complete MATLAB program, which we call `tpsplit`, is given in the Appendix.

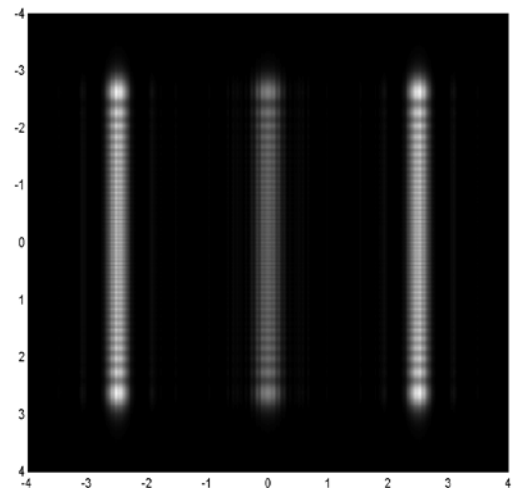
#### IV. SIMULATION RESULTS

Using the program `tpsplit`, the values of the inputs, i.e. aperture parameters  $a$  and  $b$  in mm (see Fig.2), height  $c$  in mm, image area  $W$  in mm, step size  $s$  in mm, the aperture image-

plane distance  $q_0$  in mm, the illuminating wavelength  $\lambda$  in nm and the intensity factor  $t$  are input by a GUI to the program (Fig. 5a). The intensity factor  $t$  is used to control the apparent visual intensity in the generated image. The computer generated Fresnel image due to a triple aperture for wavelength  $\lambda=500$  nm,  $q_0=400$  mm, image area  $W=4$  mm, aperture width  $a=0.5$  mm,  $b=2$  mm (with aperture separation



(a)



(b)

Fig. 5(a) Screenshot of the MATLAB GUI, showing the 8 input parameters (b) The computer simulated Fresnel image from triple aperture.

2.5mm), height  $c=3$ mm and step size  $s=0.01$ mm is shown in Fig. 5b. Three separate and distinct Fresnel diffraction patterns can be observed from each aperture, separated by a distance, with little mutual interference of the diffracted light between the three individual apertures.

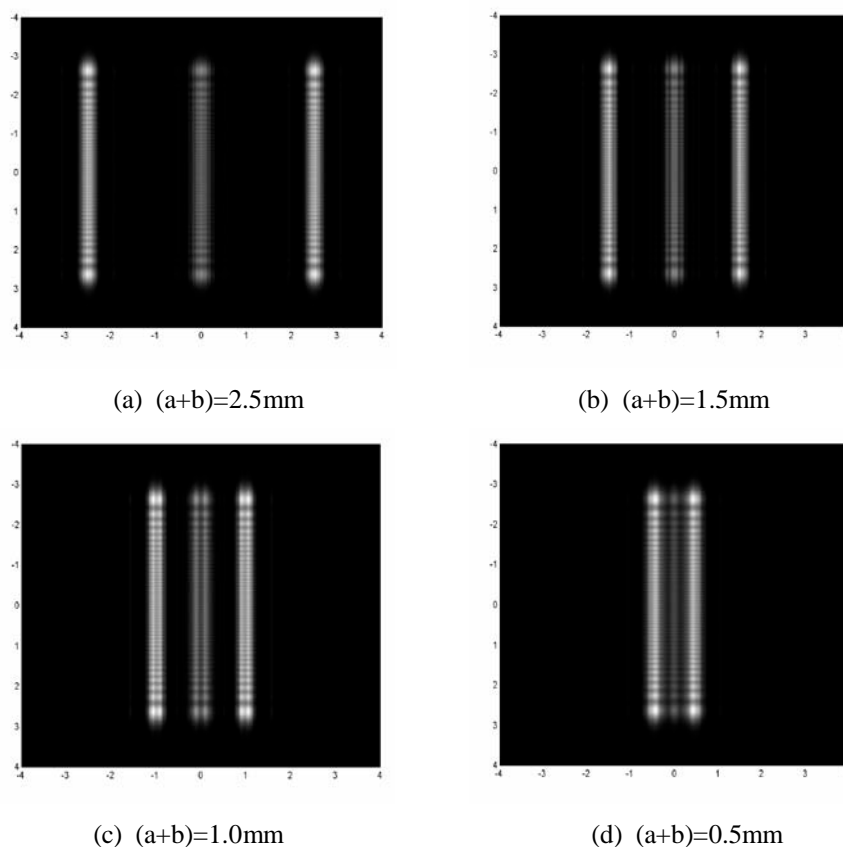


Fig. 6 Computer simulated Fresnel diffraction images for decreasing (center-to-center) aperture separation  $(a+b)$ , while keeping the aperture width  $(a=0.5 \text{ mm})$  constant. The wavelength is 500 nm, the aperture-screen distance  $q_0$  is 400 mm, step size  $s=0.01 \text{ mm}$  and  $c=3 \text{ mm}$

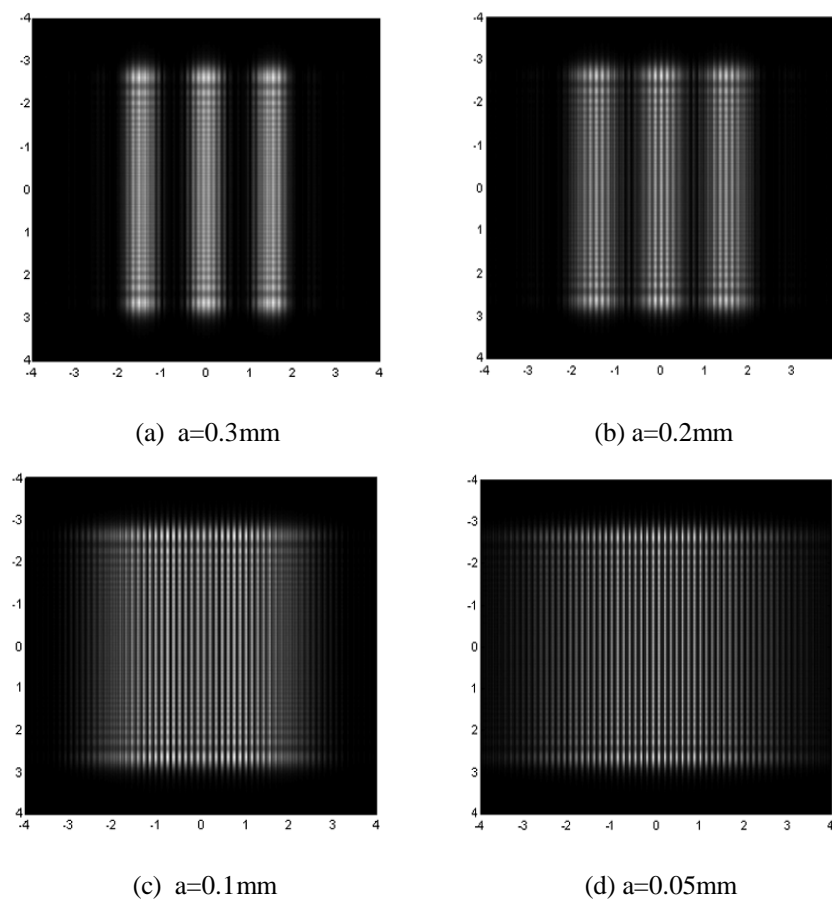


Fig. 7 Computer simulated Fresnel diffraction images for decreasing aperture width  $a$ , while keeping the aperture separation  $(a+b)$  constant at 1.5 mm. The wavelength is 500 nm, the aperture-screen distance is 400 mm, step size  $s=0.01 \text{ mm}$  and  $c=3 \text{ mm}$ .

Next, in order to examine the effect of a change of simulation parameters on the diffracted images, we have generated a series of images. In the first set of simulations, the aperture separation ( $a+b$ ) was made successively smaller, while keeping the aperture width ( $a=0.5\text{mm}$ ) constant. A series of diffraction images were simulated as shown in Fig. 6(a)-(d).

In Fig. 6(a), in the region between the apertures, there was not much interference between the light from each of the aperture diffraction patterns. But, in Fig. 6(b) and (c), some distinct interference between diffracted light from the three individual apertures has been observed as the separation of the apertures is reduced. As the separation was decreased to zero [fig. 6(d) for  $b=0$ ], a typical single aperture Fresnel diffraction pattern from an aperture of dimensions  $1.5\text{mm}\times 3\text{mm}$  has been observed.

In the next series of simulations, the width  $a$  of the apertures was made gradually narrower while their separation ( $a+b$ ) was kept constant at  $1.5\text{ mm}$ . This is shown in Fig. 7(a)-(d). From Fig. 7(a) and (b), as the apertures become narrower, the light is diffracted over a wider region and some interferences between diffracted light occur. In Fig. 7(c) and (d), at smaller aperture widths, mutual interference between diffracted light produced fringes which look like typical

Young's fringes. Light from each aperture is diffracted over a wide portion of the image area and interfere with each other. In Fig. 7(c) and (d), the density of the 'fringes' is the same, since this depends only on aperture separation.

V. COMPARISON WITH FRAUNHOFER DIFFRACTION

If the aperture-screen distance  $q_0$  is increased, a gradual transition from the Fresnel regime to Fraunhofer regime should be expected. As a rule of thumb, if  $D$  is the dimension of the square aperture, then Fresnel diffraction occurs if  $D$  satisfies the following relation [2,10] ,

$$q_0 < (D^2/\lambda). \tag{12}$$

Otherwise, Fraunhofer diffraction should occur. In the next series of simulations, we increased aperture-screen distance  $q_0$ , while keeping all other parameters constant [Fig. 8]. A transition from the Fresnel regime to Fraunhofer regime is observed, being consistent with Eq.(12). For example, in Fig. 8(a), if we take the lateral dimension to be  $D=1\text{mm}$ , then  $D^2/\lambda$  is about  $2000\text{ mm}$ , and we can expect the diffraction to be Fresnel-like in the  $y$ -direction. On the other hand, in Fig. 8(d),  $(D^2/\lambda) > q_0$ , and we can expect the diffraction pattern to be Fraunhofer-like. In between these extremes, in Fig. 8(b) and 8(c), a transition from Fresnel to Fraunhofer regime is seen to occur.

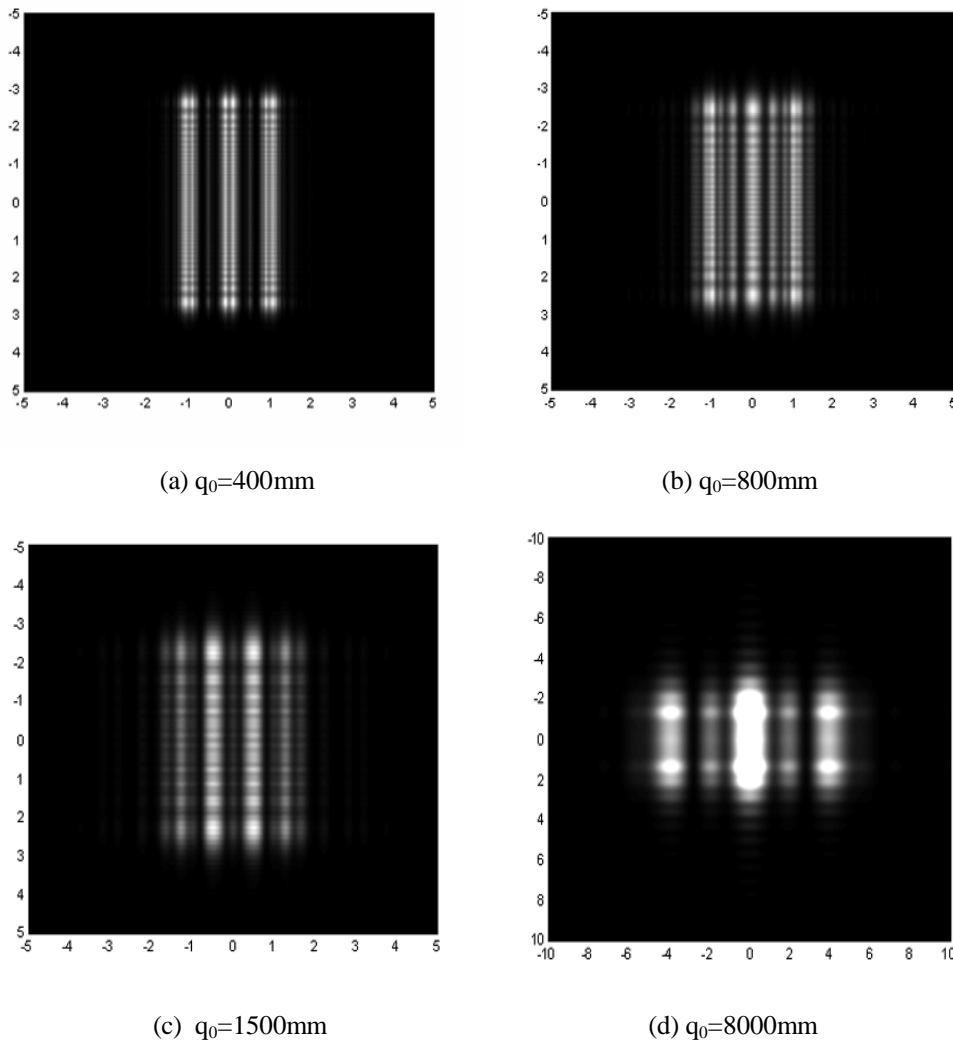


Fig. 8 Computer simulated Fresnel diffraction images for increasing aperture-screen distance  $q_0$ , while keeping all other parameters constant, with  $a=0.5\text{ mm}$ ,  $b=0.5\text{ mm}$ ,  $c=3\text{ mm}$ . The wavelength is  $500\text{ nm}$  and step size  $s=0.01\text{ mm}$ . (a) is in the Fresnel regime while (d) is in the Fraunhofer regime, according to Eq.(12)

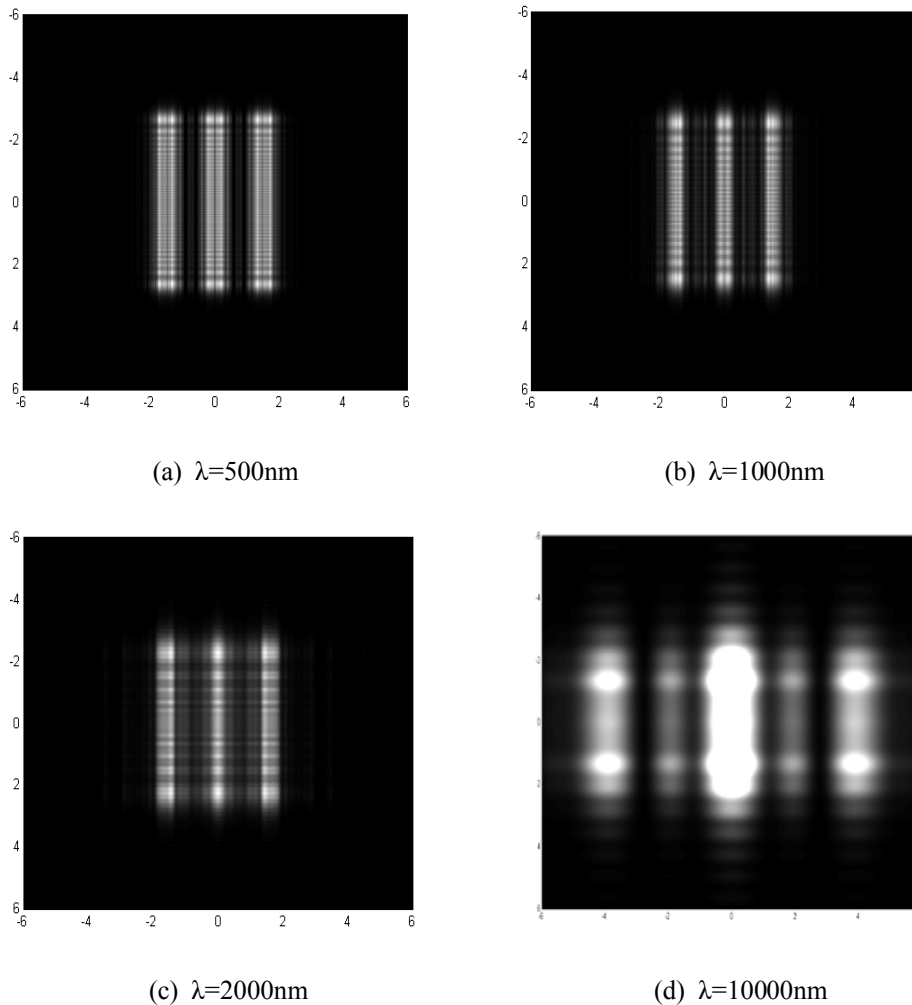


Fig. 9 Computer simulated Fresnel diffraction images for increasing wavelength  $\lambda$ , while keeping all other parameters constant, with  $a=0.5$  mm,  $b=0.5$  mm,  $c=3$  mm and  $q_0=400$  mm. (a) is in the Fresnel regime while (d) is in the Fraunhofer regime, according to Eq.(12)

By using the program `tpslit`, it is also possible to observe the effect of change of wavelength on the diffraction patterns. For example, when the wavelength was increased from 500nm (green in the visible region) to 10000nm, while keeping everything else constant in the experimental configurations (including  $q_0$ ), a transition from the Fresnel regime to Fraunhofer regime should occur, according to Eq. (12). This is shown in Fig. 9. In Fig. 9(a), the diffraction pattern is definitely Fresnel-like, while that in Fig. 9(d) is Fraunhofer-like. At intermediate wavelengths (e.g. at  $\lambda=1000$ nm and  $\lambda=2000$ nm), a transition from Fresnel to Fraunhofer regime is actually observed.

The simulated Fraunhofer diffraction image for  $q_0=8000$ mm, and an aperture dimensions  $a=0.5$ mm,  $b=0.5$  mm and  $c=1$ mm, and  $\lambda=500$ nm is shown in Fig. 10(a). For quantitative comparisons, the three dimensional mesh plot of this image is shown in Fig. 10(b), which is generated by the MATLAB `mesh` command. In this situation, the value of  $D^2/\lambda$  is 2000mm, and we expect a transition to Fraunhofer regime to occur since  $q_0$  is more than this value.

The Fraunhofer diffraction pattern of a multiple aperture in the image plane ( $Y, Z$ ) can be calculated by an analytical formula [1, 2]

$$I(Y, Z) = I_0 \left( \frac{\sin^2 \beta}{\beta^2} \right) \left( \frac{\sin^2 N\gamma}{\sin^2 \gamma} \right) \left( \frac{\sin^2 \alpha}{\alpha^2} \right). \quad (13)$$

where  $N$  is the number of apertures ( $N=3$  in our case) and  $\beta, \gamma$  and  $\alpha$  are defined as,

$$\beta = \frac{\pi}{\lambda} a \frac{Y}{R}, \quad \gamma = \frac{\pi}{\lambda} (a+b) \frac{Y}{R}, \quad \alpha = \frac{\pi}{\lambda} c \frac{Z}{R}. \quad (14)$$

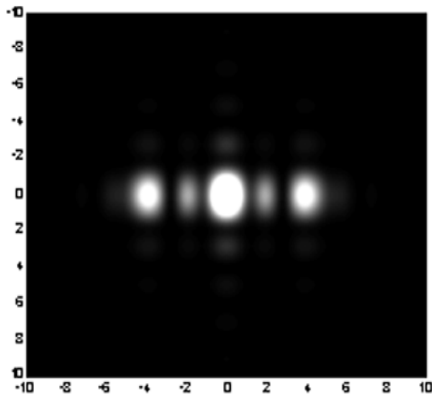
In the above equations,  $a$  is aperture width,  $(a+b)$  is the aperture separation,  $c$  is aperture height,  $\lambda$  is the wavelength and  $R$  is the distance between the aperture and the screen, assumed to be very large. Using Eq. (13), a MATLAB program was written to compute the intensity distribution in the image plane, which accepts the values of  $a, b, c$ , distance  $R$ , wavelength  $\lambda$  and the desired image area  $2W \times 2W$ . The intensity can be shown, for quantitative comparisons, as a mesh plot by MATLAB. The mesh plot is shown in Fig. 10(c) considering the above parameters.

Comparing Fig. 10(b) and 10(c), a fair agreement can be observed, including the minor peaks. This means that the simulation method of Fresnel diffraction for triple aperture is correct, since it has a good quantitative match with a purely Fraunhofer calculation under similar conditions, i.e. at large

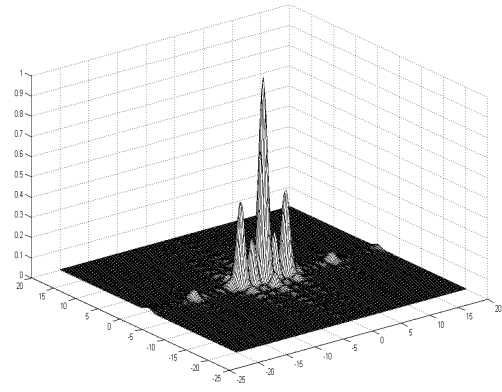
aperture-screen distance,  $q_0$ . The slight difference between Fig. 10(b) and 10(c) may be attributed to the fact that Eq. (13) is valid for extremely large distances, but in reality the distance is 8000mm only.

To test this assumption, we have generated another computer simulation by our program for the above situation, but with a larger value of  $q_0$  (20,000mm). The intensity distribution and mesh plot are shown in Fig. 11(a) and 11(b).

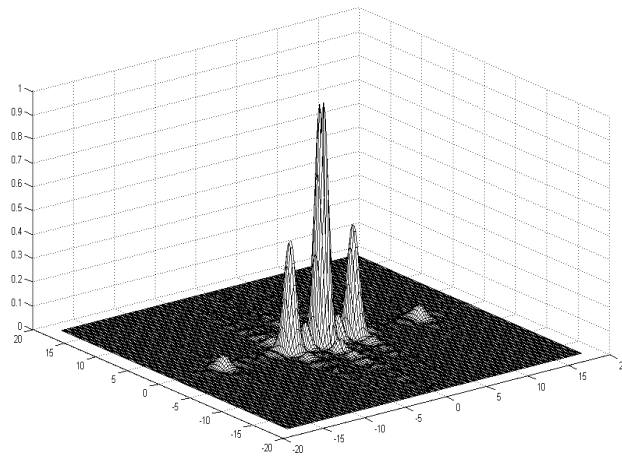
Fig. 11(c) shows the mesh plot of the intensity distribution calculated by the Fraunhofer formula [Eq. 13] for  $q_0=20,000$  mm. In this case, a better agreement between Fig. 11(b) and Fig. 11(c) can be clearly seen. This means that as  $q_0$  becomes larger and larger, the agreement between the simulation results by IFIM method and the Fraunhofer formula becomes better and better.



(a)

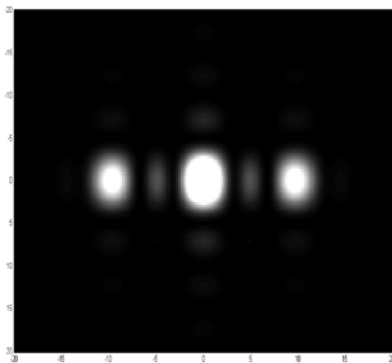


(b)

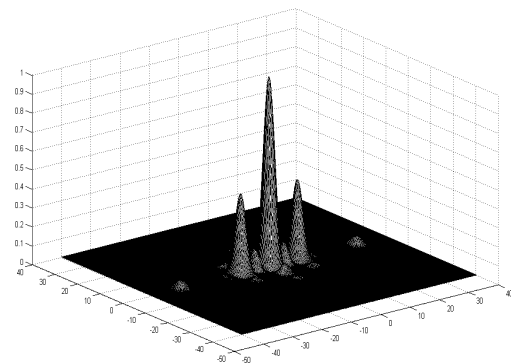


(c)

Fig. 10 (a) Computer simulated far-field diffraction images for the triple aperture, with  $a=0.5$  mm,  $b=0.5$  mm,  $c=1$  mm,  $\lambda=500$  nm and  $q_0=8000$  mm (Fraunhofer limit). (b) Mesh plot of the far-field diffraction pattern for this aperture. (c) Mesh plot of the far-field diffraction pattern for this aperture generated by the Fraunhofer formula.

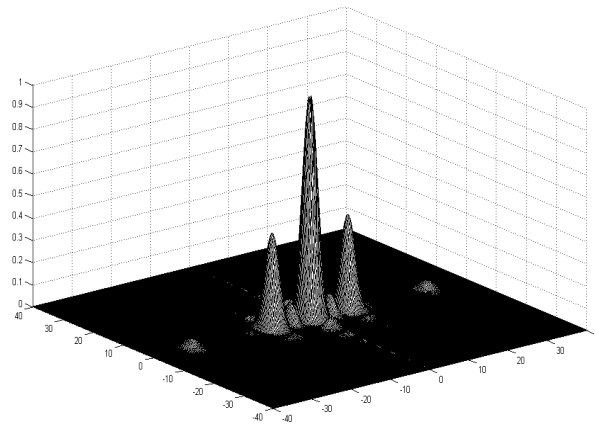


(a)



(b)





(c)

Fig. 11 (a) Computer simulated far-field diffraction images for the triple aperture, with  $a=0.5$  mm,  $b=0.5$  mm and  $c=1$  mm,  $\lambda=500$  nm and  $q_0=20,000$  mm (Fraunhofer limit). (b) Mesh plot of the far-field diffraction pattern for this aperture. (c) Mesh plot of the far-field diffraction pattern generated by the Fraunhofer formula.

VI. DISCUSSION

In this paper, we have described a method to calculate and simulate the complete Fresnel diffraction image of the triple aperture using the Iterative Fresnel Integrals Method. Though not as popular as the double aperture or slit, the triple slit has been used as the source of interference in a triple-slit interferometer [11]. Each of our simulations is a virtual experiment, where the results of performing a real diffraction experiment can be obtained purely by simulation, without actually performing it.

The theoretical background as well as the complete implementation of the algorithm in MATLAB codes is given in this paper. We have computed first the complex electric field distribution in the image plane, and then calculated the intensity distribution by squaring it. Here we have used the complex number capability of MATLAB to full advantage. This affords some simplification in the computation process.

In Eq. (2) or Eq. (3), it was tacitly assumed that the obliquity factor  $K(\phi)$  is unity for all waves emitted from all the surface elements  $dS$  located inside the triple aperture. But actually, in our simulations, in order to calculate the electric fields at an arbitrary point P' in the image plane, we virtually translated the triple aperture in the  $y$  and  $z$  directions and calculated the electric field at the origin P of the image plane (see, for example, Figs. 2 and 4). These translations of the aperture effectively make the light emitted from the aperture slightly non-paraxial (off-axis). As an example, [in the simulation of Fig. 5], for an image area  $W=4$  mm, aperture-screen distance  $q_0=400$ mm, and with aperture dimensions  $a=0.5$ mm,  $b=2$ mm,  $c=3$ mm, the extreme off-axis waves will be emitted from surface elements  $dS$  located at  $y=W+3a/2+b$  and at  $z=W+c$ , for virtual translations  $W$  of the aperture in the  $y$  and  $z$ -directions, respectively (see, for example, Fig. 4). For these waves, the maximum values of  $\phi$  are  $(W+3a/2+b)/q_0$  and  $(W+c)/q_0$ , respectively, and work out to be about 1 degree in both cases. The corresponding value of the obliquity factor  $K(\phi) [=1/2(1+\cos \phi)]$  is about 0.99992, and can be taken equal to unity, as was done in Eq. (2) and Eq. (3). This approximation produces a maximum error of less than 0.01% in the calculation of electric fields. For larger image areas, larger apertures, or smaller aperture-screen distances,  $\phi$  would

be correspondingly larger. To limit the error in  $K(\phi)$  (and hence in the electric field) to less than 1%, the maximum allowed value of  $\phi$  should be about 10 degrees. This probably covers most cases of practical interest.

For the simulations, we used an office computer using an Intel core-i7 CPU having 4GB of RAM running at a clock speed of 3.4GHz under Windows 7. The simulation time for a typical 1000X1000 pixel image is about 10 seconds. For slower computers or for larger images, the simulation time may be significantly greater.

Using the program, we simulated the Fresnel diffraction in a number of situations. We have found that as the individual apertures of the triple aperture are brought closer, significant interference between diffracted light can be seen in the region between the apertures. On the other hand, if the aperture widths of the individual aperture are made narrower while keeping their separation constant, then the light is diffracted over a wider region. Interference effects with the light diffracted from the apertures can be seen, and Young-like fringes appear on the image plane.

The expected transition from Fresnel to Fraunhofer regions can also be observed under appropriate conditions. For example, when the aperture-screen distance  $q_0$  is increased, or when the wavelength  $\lambda$  is increased, a transition from Fresnel regime to Fraunhofer regime is actually observed. In addition, good quantitative agreement was observed between the simulated Fresnel diffraction pattern at large aperture-screen distances (in the Fraunhofer regime) and the intensity distribution generated by an analytical Fraunhofer formulation. This agreement becomes better as the aperture-screen distance is increased more, and provides a proof that our simulation method is correct and appropriate.

VII. CONCLUSION

In conclusion, we have described a method to compute and generate, in virtually any PC, the complete near-field Fresnel diffraction patter from a triple aperture in any arbitrary experimental configuration by the Iterative Fresnel Integrals Method. This simulation and virtual experiment provide a simple and easy-to-use method to study the complex phenomenon of diffraction from a triple aperture system.

ACKNOWLEDGMENT

One of the authors (KMA) would like to thank the Sultan Qaboos University for inviting him as a Visiting Consultant of the Department of Physics during the Spring 2012 Semester.

REFERENCES

[1] F.A. Jenkins and H.E. White, *Fundamentals of Optics*, 4th ed., New York: McGraw-Hill, 1976. [chapter 15, p. 315].  
 [2] E. Hecht, *Optics*, 4th ed., Singapore: Pearson Education, 2002.[chapter 10].  
 [3] M. Born and E. Wolf, *Principles of Optics*, 7th ed., Cambridge: Cambridge University Press, 1999. [chapter 8].  
 [4] K.M. Abedin, M.R. Islam, and A.F.M.Y. Haider, "Computer simulation of Fresnel diffraction from rectangular aperture and obstacles using the Fresnel integrals approach," *Opt. Laser Technol.*, Vol. 39, 237, 2007.  
 [5] K.M. Abedin and S.M.M. Rahman, "Computer simulation of Fresnel diffraction from double rectangular aperture in one and two dimensions using the iterative Fresnel integrals method," *Opt. Laser Technol.*, Vol. 44, 394, 2012.  
 [6] K.M. Abedin and S.M.M. Rahman, "The iterative Fresnel integrals method for Fresnel diffraction from tilted rectangular: Theory and simulations," *Opt. Laser Technol.*, Vol. 44, 939, 2012.  
 [7] R.G. Wilson, S.M. McCreary and J.L. Thompson, "Optical transforms in three-space: Simulations with a PC," *Am. J. Phys.* Vol. 60, 49, 1992.  
 [8] D.E. Dager, "Simulation and study of Fresnel diffraction for arbitrary two-dimensional apertures," *Comput. Phys.* Vol. 10, 591, 1995.  
 [9] S. Trester, "Computer-simulated Fresnel diffraction using the Fourier transform," *Comput. Sci. Eng.*, Vol. 1, 77, 1999.  
 [10] S.G. Lipson, H. Lipson and D.S. Tannhauser, *Optical Physics*, 3rd ed. Cambridge: Cambridge University Press, 1995. [Chap. 7, p.162].  
 [11] Y. B. Ovchinnikov, "Fresnel interference pattern of a triple-slit interferometer," *Opt. Commun.* Vol. 216, 33, 2003.

APPENDIX

**tpsplit: Complete MATLAB program for the triple aperture**

```

1.u=inputdlg({'a mm','b mm','c mm','W mm','s mm','
            q0 mm','l nm',...
2.'exposure'},'Fresnel Diffraction from triple aperture',
            [1,1,1,1,1,1,1,1]);
3.for i=1:8; v(i)=str2num(u{i}); end
4.q0=v(6); t=v(8); l=v(7)*1e-6; f=sqrt(2/(l*q0));
5.a=v(1)*f; b=v(2)*f; c=v(3)*f; W=v(4)*f; s=v(5)*f;
6.Cu2=mfun('FresnelC',3/2*a+b:s:W+3/2*a+b);
7.Cu1=mfun('FresnelC',a/2+b:s:W+a/2+b);
8.Cu4=mfun('FresnelC',a/2:s:W+a/2);
9.Cu3=mfun('FresnelC',-a/2:s:W-a/2);
10.Cu6=mfun('FresnelC',-a/2-b:s:W-a/2-b);
11.Cu5=mfun('FresnelC',-3/2*a-b:s:W-3/2*a-b);
12.Su2=mfun('FresnelS',3/2*a+b:s:W+3/2*a+b);
13.Su1=mfun('FresnelS',a/2+b:s:W+a/2+b);
14.Su4=mfun('FresnelS',a/2:s:W+a/2);
15.Su3=mfun('FresnelS',-a/2:s:W-a/2);
16.Su6=mfun('FresnelS',-a/2-b:s:W-a/2-b);
17.Su5=mfun('FresnelS',-3/2*a-b:s:W-3/2*a-b);
18.A=complex(Cu2+Cu4+Cu6-Cu1-Cu3-
            Cu5,Su2+Su4+Su6-Su1-Su3-Su5);
19.Cv2=mfun('FresnelC',c:s:W+c);
20.Cv1=mfun('FresnelC',-c:s:W-c);
21.Sv2=mfun('FresnelS',c:s:W+c);
22.Sv1=mfun('FresnelS',-c:s:W-c);
23.B=complex(Cv1-Cv2,Sv1-Sv2);
24.B=B';n=size(B);B= repmat(B(:,1),1,n);
25.A=A';A= repmat(A(:,1),1,n);A=(A)';
26.C=B*A;D=C.*conj(C);
    
```

```

27.D=t*D/max(max(D));
28.m=2*fix(((2*W)/s)/2);
29.E=zeros(m+1,m+1);
30.for q=1:1:m/2+1;
31.for p=1:1:m/2+1; E(m/2+2-p,q+m/2)=D(p,q); end
32.end
33.for q=m+1:-1:m/2+2;
34.for p=1:1:m/2+1;E(p,-q+2+m)=E(p,q);end
35.end
36.for q=1:1:m+1;
37.for p=1:1:m/2;E(-p+2+m,q)=E(p,q);end
38.end
49.y=-W:s:W;ymm=y/f;
40.imageesc(ymm,ymm,E,[0,1]);colormap(gray);
    
```

**Fatema Hamid Al-Saiari** is a final year B.Sc. student in the Sultan Qaboos University, Muscat, Oman, majoring in physics. She was born in Salalah, Oman in 1988. She enrolled in Sultan Qabbos University in 2006, and is expected to graduate in 2012. The present work is based on her B.Sc. project.

**S. M. Mujibur Rahman** is a Professor and the Head of the Department (HoD) of Physics, College of Science, Sultan Qaboos University, Muscat, Oman. He was born in Dhaka, Bangladesh, in 1951. He obtained his B.Sc. (honours) degree in 1972 in the First Class from the Department of Physics, University of Dhaka, Bangladesh. He obtained his M. Sc. Degree, also in the First Class, from the same Department in 1973. He obtained his Ph.D. degree in theoretical condensed matter physics from the University of Dhaka in 1979, and also from the University of Bristol, UK, in the same year.

He became a Lecturer in 1975, Assistant Professor in 1979, Associate Professor in 1982 and a full Professor in 1988, all in the Department of Physics, University of Dhaka. He has been an Alexander von Humboldt Fellow in Germany, Nuffield Fellow of the Royal Society, UK, and a Senior Associate of ICTP, Italy. In 1989, he joined the Physics Department of Sultan Qaboos University, Oman, where he is presently a full Professor and the Head of the Department. His research interests include structural, thermodynamic, and transport properties of metals, binary alloys, and amorphous systems. He is also involved with the magnetic properties of materials, dynamics of hydrocarbon fluids, atomic diffusion in materials, and diffraction theory of light. He is the author or co-author of about 80 peer-reviewed journal publications.

Professor Rahman is a life member of the Bangladesh Physical Society, the New York Academy of Sciences and the Asian Physical Society. He is the recipient of many awards, including the Bangladesh Academy of Science Gold Medal and the A.R. Chowdhury Gold Medal. He has been a member of the Editorial Board of the SQU Journal of Science and is presently a member of the Editorial Board of the International Journal of Pure and Applied Physics (Delhi).

**Kazi Monowar Abedin** is a Professor of Physics in the University of Dhaka, Bangladesh. He was born in Dhaka in 1963. He obtained his B.Sc. (honours) degree in 1987 in the First Class from Department of Physics, University of Dhaka, Bangladesh, securing first position in order of merit in his class. He earned his M.S. degree in Applied Physics from the University of Tsukuba, Japan in 1991, and his Ph.D. degree in Engineering (laser spectroscopy) from the same university in 1994. His Ph.D. thesis concerned with the ultrafast subpicosecond dynamics of dye molecules doped in organic hosts.

He joined the faculty of University of Dhaka in 1994 as an Assistant Professor. He became an Associate Professor in 2000, and a full Professor in 2003 there. He was an STA (Science and Technology Agency) Fellow in the Mechanical Engineering Laboratory, Tsukuba, Japan during the years 1996-97. In addition, he was a Commonwealth Fellow in the Clarendon Laboratory, University of Oxford, UK, during 2001-2002, and a Visiting Professor at Tohoku University, Sendai, Japan, during 2006-2007. He was a Guest Scientist at the Max Planck Institute for the Science of Light, in Erlangen, Germany during 2008-2009. He served as a Visiting Consultant in the Physics Department of Sultan Qaboos University, Oman, in 2011 and 2012. His present and past research interests include laser-induced breakdown spectroscopy (LIBS), laser Raman spectroscopy, laser remote sensing, diffraction theory of light, optical speckle metrology (ESPI) and optical interferometry, ultrafast laser spectroscopy, physics of laser devices, and solid-state dye lasers. He is the author or co-author of 3 book chapters and more than 40 peer-reviewed journal publications.

Professor Abedin is a life member of the Bangladesh Physical Society. He is the recipient of several awards, including the Ibrahim Memorial Gold Medal and the Razaq-Shamsun Research Prize.